ICSV14
Cairns • Australia
9-12 July, 2007

14th International Congress on Sound & Vibration

VALIDATION OF AN INNOVATIVE HYBRID METHOD FOR THE PREDICTION OF NOISE GENERATED BY CONFINED FLOWS

Christophe Schram[1]*, Michel Tournour[1]†

[1]CAE Division
LMS International
Interleuvenlaan 68
Researchpark Haasrode Z1
3001 Leuven
Belgium

*christophe.schram@lms.be
†michel.tournour@lms.be

Abstract

In this work we are concerned with noise generation by confined flows: HVAC systems, automotive exhaust systems (mufflers), and industrial fluid distribution systems.

We are aiming at predicting the generation and propagation of flow-induced noise in ducts with arbitrary geometries, and for frequencies high enough for transverse modes to be cut-on. Curle's analogy was shown to perform poorly in such configurations, when applied using incompressible or low-order compressible CFD data as input. We have developed an innovative hybrid method, based on the combination of Curle's analogy with a Boundary Element Method, to compensate for the weaknesses of Curle's analogy in such applications. The originality of the method stands in its decoupling between hydrodynamic and acoustical informations at the wall.

This method is validated by application to a test case: the sound emitted by a co-rotating pair of vortex filaments leapfrogging in an infinite 2D duct. Our results show a remarkable agreement with a reference solution based on the duct modes, thereby validating our approach.

1. AEROACOUSTICAL ANALOGY

We consider the original analogy derived by Lighthill [1] for the sound generated by free turbulence at low Mach numbers, and its generalisation by Curle [2] to account for the noise resulting of turbulence interacting with solid steady surfaces.

Upon definition of a reference thermodynamic state (ρ_0, p_0) uniform in time and space in a propagation region, Lighthill's analogy describes the propagation of acoustical density perturbations $\rho' \equiv \rho - \rho_0$ at the speed of sound $c_0 = \sqrt{(\partial p/\partial \rho)_S}$ in an homogeneous acoustic medium, emitted by the equivalent source $\partial^2 T_{ij}/\partial x_i \partial x_j$:

$$\frac{\partial^2 \rho'}{\partial t^2} - c_0^2 \frac{\partial^2 \rho'}{\partial x_i^2} = \frac{\partial^2 T_{ij}}{\partial x_i \partial x_j} \tag{1}$$

where $T_{ij} = \rho v_i v_j + (p' - c_0^2 \rho') \delta_{ij} - \sigma_{ij}$ is the Lighthill stress tensor accounting for the sound production by Reynolds stresses, non-isentropic processes and viscous stresses [1].

The wave propagation equation can be integrated in time and space by convolution with a free field Green's function $G_0(t, \mathbf{x}|\tau, \mathbf{y})$, solution of the wave propagation equation with an impulsive source emitted at the position $\mathbf{y}$ and time τ. This consists in propagating a source term behaving as a monopole, to be scattered by the solid boundaries. We will show below that this straightforward method is hampered by numerical robustness issues. A more sensible approach proposed by Curle [2] consists in integrating by parts the integral of the source field, leading to the well-known result:

$$\rho'(\mathbf{x}, t) = \int_{-\infty}^{t} \iiint_V \rho_0 v_i v_j \frac{\partial^2 G_0}{\partial y_i \partial y_j} \, \mathrm{d}^3\mathbf{y} \mathrm{d}\tau - \int_{-\infty}^{t} \iint_{\partial V} p' \frac{\partial G_0}{\partial y_i} n_i \, \mathrm{d}^2\mathbf{y} \mathrm{d}\tau \tag{2}$$

where the presence of the solid boundary appears through the dipole sources distributed over its surface ∂V. Though exact from a formal viewpoint, the derivation that leads to Eq. (2) introduces the assumption that the flow model does account for scattering effects. Our experience shows that this assumption is not valid for non-compact configurations as considered in this work, especially when incompressible flow modeling is involved. Indeed, if the pressure fluctuation induced at the wall by nearby turbulence does effectively account for near-field scattering, the pressure component that is radiated by remote sources is usually not accounted for when using incompressible or low-order compressible flow simulations, especially when resolved over unstructured meshes, at low Mach numbers. The approach based on Eq. (2) is still valid as long as the source region is acoustically compact, because scattering is of negligible importance on the one side, and because the acoustical effects for low Helmholtz numbers can be approximately captured by an incompressible modeling on the other side. But for non-compact cases, the incompressible flow model must be complemented by an acoustic correction to obtain a realistic sound prediction. A straightforward alternative could consist in adopting for Eq. (2) a Green's function G_1 tailored to the geometry, i.e. having zero normal gradient at the boundary surface, instead of the free field Green's function G_0:

$$\rho'(\mathbf{x}, t) = \int_{-\infty}^{t} \iiint_V \rho_0 v_i v_j \frac{\partial^2 G_1}{\partial y_i \partial y_j} \, \mathrm{d}^3\mathbf{y} \mathrm{d}\tau \, . \tag{3}$$

This tailored Green's function G_1 accounts then for the scattering that was missed by the flow model, in addition to the incident field that was given by the Green's function G_0. A comparison of Eq. (2) and Eq. (3) shows that the surface integral of Eq. (2) represents the scattered field:

$$- \int_{-\infty}^{t} \iint_{\partial V} p' \frac{\partial G_0}{\partial y_i} n_i \, \mathrm{d}^2\mathbf{y} \mathrm{d}\tau = \int_{-\infty}^{t} \iiint_V \rho_0 v_i v_j \frac{\partial^2 G_S}{\partial y_i \partial y_j} \, \mathrm{d}^3\mathbf{y} \mathrm{d}\tau \tag{4}$$

where the Green's function $G_S = G_1 - G_0$ yields the scattered field (total field $-$ incident field).

Tailored Green's functions are however only known for a quite limited number of idealized cases, using mirror images of the sources for example in presence of infinite planes, or calculated by separation of variables when the geometry is aligned with orthogonal directions of a suitable coordinate system. For low frequencies, analytical approximations can be considered, such as Howe's compact Green's functions [3]. In most industrial applications and range of frequencies however, the problem is not amenable to an analytical solution, and one must resort to a numerical treatment. For internal problems, building a numerical Green's function based on numerical acoustic modes is possible in theory, but the handling of this function depending on the frequency, emitter and listener positions is not achievable in practice. We propose in next Section an original approach, combining Curle's analogy with a Boundary Element Method, to bring the acoustical correction needed when using incompressible flow data at medium to high Helmholtz numbers.

2. BOUNDARY INTEGRAL FORMULATION OF CURLE'S ANALOGY

The derivation of the boundary integral formulation follows the same approach as Curle's analogy. The inhomogeneous wave propagation equation is usually expressed in frequency domain in the form of the Helmholtz equation $\nabla^2 \hat{p}_\mathrm{a} + k^2 \, \hat{p}_\mathrm{a} = \hat{q}_\mathrm{L}$ where $c_0^2 \rho' = p'_\mathrm{a} = \hat{p}_\mathrm{a} \, \mathrm{e}^{\mathrm{i}\omega t}$, and $k = \omega / c_0$, $\hat{q}_\mathrm{L} = -\partial^2 \hat{T}_{ij} / \partial x_i \partial x_j$ with $T_{ij} = \hat{T}_{ij} \, \mathrm{e}^{\mathrm{i}\omega t}$. The Helmholtz Equation (2) is solved using a free field Green's function $G_0 = \mathrm{e}^{-\mathrm{i}kr}/(4\pi r)$ solution of the equation $\nabla^2 G_0 + k^2 \, G_0 = -\delta \, (\mathbf{x} - \mathbf{y})$ in absence of solid surfaces. Dropping the hat notations, one obtains:

$$\iiint_{V \setminus V_\varepsilon} \left(\nabla^2 p_\mathrm{a} \, G - p_\mathrm{a} \, \nabla^2 G \right) \mathrm{d}^3\mathbf{y} = \iiint_{V \setminus V_\varepsilon} q_\mathrm{L} G \, \mathrm{d}^3\mathbf{y} + \iiint_{V \setminus V_\varepsilon} p_\mathrm{a} \, \delta \, (\mathbf{x} - \mathbf{y}) \, \mathrm{d}^3\mathbf{y} \qquad (5)$$

with however a significant difference compared to Curle's analogy: an exclusion volume V_ε including the listener's position $\mathbf{x}$ was removed from the integration volume V, in order to apply Green's theorem. The exclusion volume was not necessary in the derivation of Curle's analogy, because in the classical aeroacoustical analogy the listener is implicitly situated in the propagation region, defined well apart from the source field. At the opposite, the resolution of the BEM model is performed by collocation, i.e. by placing the listener directly on the nodes of the boundary surface, thereby introducing a singularity in the integration volume. This singularity is excluded by removing the volume V_ε from the source integration, and its contribution will be evaluated by letting V_ε shrink to zero volume. The point $\mathbf{x}$ being excluded from the integration volume $V \setminus V_\varepsilon$, the contribution of the third integral of Eq. (5) is equal to zero.

Applying Green's theorem, we find:

$$C(\mathbf{x}) \, p_\mathrm{L}(\mathbf{x}) = \iiint_V T_{ij} \, \frac{\partial^2 G}{\partial y_i \partial y_j} \, \mathrm{d}^3\mathbf{y} - \iint_{\partial V} p_\mathrm{L} \, \frac{\partial G}{\partial n} \, \mathrm{d}^2\mathbf{y} \qquad (6)$$

where the pressure p_L comes from the Lighthill's tensor, irrespectively of any acoustic or hydrodynamic discrimination, at the difference of the pressure p_a. The factor $C(\mathbf{x})$ is the solid angle seen by the point $\mathbf{x}$ in the exclusion volume V_ε divided by 4π, i.e. equal to 1 when $\mathbf{x}$ is within the volume, and equal to 1/2 when $\mathbf{x}$ lies over a smooth surface of the body.

Equation (6) is quite similar to the result derived in the classical analogy of Curle (2), up to differences related to the change from time to frequency domain, including the factor c_0^2 due to the different Green's functions in time and frequency domains. A remarkable difference, however, is that Eq. (6) does resolve the pressure fluctuations whatever their hydrodynamic or acoustical nature, while Eq. (2) yields the acoustical pressure $p_\mathrm{a} = c_0^2 \rho'$ in the propagation region only. This results from having allowed the listener to enter the source region, while in Curle's analogy the listener is always assumed as located in a uniform and quiescent propagation region. As a corollary, Eq. (2) provides an explicit solution for the acoustic field, while Eq. (6) can be seen as an implicit integral equation giving the pressure at any point of the flow field, including at the body surface, provided the volumetric term is known.

In line with the discussion of previous Section, we argue that an exact flow description will always satisfy Eq. (6), while an incompressible flow model will only verify the same relation if the domain V is acoustically compact, i.e. if acoustical propagation is irrelevant. In such case, the pressure on both sides of Eq. (6) can be approximated by its incompressible, hydrodynamic component: $p_\mathrm{L} \simeq p_\mathrm{h}$. In a more general case, we let the pressure be expressed as the sum of a hydrodynamic and an acoustic component: $p_\mathrm{L} = p_\mathrm{h} + p_\mathrm{a}$. Besides, we decompose the integration domain of (6) in two parts, corresponding respectively to volumes V_1 and V_2, and their boundaries ∂V_1 and ∂V_2, as indicated in Figure 1:

$$\begin{aligned} C(\mathbf{x})\ (p_\mathrm{h}(\mathbf{x}) + p_\mathrm{a}(\mathbf{x})) = & \iiint_{V_1} T_{ij} \frac{\partial^2 G}{\partial y_i \partial y_j} \,\mathrm{d}^3\mathbf{y} - \iint_{\partial V_1} (p_\mathrm{h} + p_\mathrm{a}) \frac{\partial G}{\partial n} \,\mathrm{d}^2\mathbf{y} \\ & + \iiint_{V_2} T_{ij} \frac{\partial^2 G}{\partial y_i \partial y_j} \,\mathrm{d}^3\mathbf{y} - \iint_{\partial V_2} (p_\mathrm{h} + p_\mathrm{a}) \frac{\partial G}{\partial n} \,\mathrm{d}^2\mathbf{y} \end{aligned} \quad (7)$$

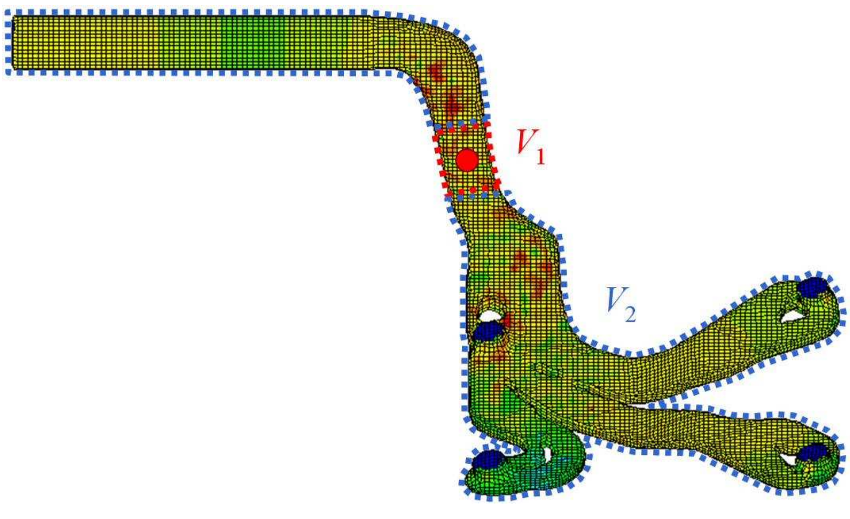

Figure 1. Typical HVAC duct: collocation node (in red) and definition of the volumes V_1 and V_2. At the collocation node, we decompose the wall pressure into a near-field component due to the scattering of turbulence in V_1, and the scattering of an acoustic component radiated by remote turbulence in V_2.

The domain V_1 is localized around the collocation point $\mathbf{x}$, with dimensions proportional to the local turbulence correlation length, i.e. acoustically compact at low Mach numbers. The domain V_2 is defined as $V \setminus V_1$. It was argued above that the hydrodynamic pressure is solution of Eq. (6) with $p_\mathrm{L} \simeq p_\mathrm{h}$ over the compact domain V_1:

$$C(\mathbf{x})\, p_\mathrm{h}(\mathbf{x}) = \iiint_{V_1} T_{ij} \frac{\partial^2 G}{\partial y_i \partial y_j}\, \mathrm{d}^3\mathbf{y} - \iint_{\partial V_1} p_\mathrm{h} \frac{\partial G}{\partial n}\, \mathrm{d}^2\mathbf{y} \tag{8}$$

Subtracting Eq. (8) from Eq. (7) yields:

$$\begin{aligned} C(\mathbf{x})\, p_\mathrm{a}(\mathbf{x}) &= -\iint_{\partial V_1} p_\mathrm{a} \frac{\partial G}{\partial n}\, \mathrm{d}^2\mathbf{y} + \iiint_{V_2} T_{ij} \frac{\partial^2 G}{\partial y_i \partial y_j}\, \mathrm{d}^3\mathbf{y} - \iint_{\partial V_2} (p_\mathrm{h} + p_\mathrm{a}) \frac{\partial G}{\partial n}\, \mathrm{d}^2\mathbf{y} \\ &= -\iint_{\partial V} p_\mathrm{a} \frac{\partial G}{\partial n}\, \mathrm{d}^2\mathbf{y} + \iiint_{V_2} T_{ij} \frac{\partial^2 G}{\partial y_i \partial y_j}\, \mathrm{d}^3\mathbf{y} - \iint_{\partial V_2} p_\mathrm{h} \frac{\partial G}{\partial n}\, \mathrm{d}^2\mathbf{y} \end{aligned} \tag{9}$$

where the boundary integrals involving the acoustical pressure p_a have been grouped together.

The wall pressure can therefore be expressed as the sum of a hydrodynamic component, which can be obtained by an incompressible flow model, and an acoustical component, solution of Eq. (9). This integral implicit equation can be classically resolved using a boundary element method, considering the two last integrals as an incident field. Once the acoustic component of the wall pressure field has been obtained, it must be summed up with the hydrodynamic component to yield the complete dipolar source term of Curle's analogy.

The formulation (9) has been implemented in the boundary element solver of the commercial code SYSNOISE Rev 5.6, which was used to generate the results shown below. The details of the implementation would be too lengthy to be included here, but an extensive description of the basics and numerical implementation of the boundary element method can be found in [4].

3. RESULTS

The approach has been tested by application to a two-dimensional benchmark problem. We consider the sound produced by the leapfrogging of two filament vortices within an infinite two-dimensional straight duct. This benchmark permits a quasi-analytical derivation of the flow field and sound production.

3.1. Flow model and acoustic sources

The two vortices are initially placed at the centreline of a duct with unit height h, have a circulation $\Gamma = 85\ \mathrm{m^2\,s^{-1}}$, and are spaced in the longitudinal direction by a distance $d = h/2$. The characteristic Mach number is therefore $M = \Gamma/(d\,c_0) = 0.5$ with a speed of sound $c_0 = 340\ \mathrm{m\,s^{-1}}$.

The velocity of each vortex filament is obtained analytically by derivation of the complex potential associated with the two vortices and their respective infinite rows of image vortices due to the presence of the non-viscous walls. In this benchmark, we apply an incompressible flow model (pointwise Biot-Savart induction) to obtain the unsteady flow field, which may be questionable at a Mach number of 0.5. The error due to compressibility effects scales however with the square of the Mach number [5]. Besides, the rational for using such large Mach number is to obtain a flow field radiating sound at frequencies above the cut-off frequency of the duct.

The positions of the two vortices at each time step are integrated using the ODE45 Runge-Kutta solver of Matlab 6.5. In order to remove the velocity singularity at the centre of the vortices, the velocity field over the whole duct section has been calculated by patching, at each time step, Oseen angular velocity distributions $v_\theta = \Gamma/(2\pi r)\left(1 - \mathrm{e}^{-r^2/(2\sigma^2)}\right)$, with a vortex core size chosen equal to twice the mesh resolution (uniform in both x, y directions). It was verified that this desingularization of the vortex cores does not yield a significant error in the prediction of the sound production [6].

The unsteady velocity fields have then been post-processed to calculate the Lighthill's tensor $T_{ij} \simeq \rho_0 v_i v_j$ in two-dimensions. The wall pressure has been obtained by applying the unsteady Bernoulli's equation following the streamlines aligned with each wall from infinity to the source region. Both surface and line source terms have been Fourier-transformed for use in the BEM solver of SYSNOISE Rev 5.6 The details about the derivations are given in full length by Schram [6].

3.2. Sound prediction

Figure 2 below shows several acoustical results, for a frequency of 261 Hz ($k\,h = 4.8$). Figure 2(a) shows the sound pressure field obtained by using a tailored Green's function, according to Eq. (3). The tailored Green's function is obtained on the basis of the duct modes, matched at the source location, as shown by Schram [6]. This is considered as the reference, exact solution, up to the approximations of the source field described above.

Figure 2(b) shows the sound prediction obtained using our innovative formulation (9). While it was shown by Schram [7] that a straightforward application of Curle's classical analogy yields completely erroneous results for this benchmark, it is now demonstrated that our method yields excellent agreement with the reference data. A few discrepancies are found in the near field of the source region, which can probably be attributed to the poor convergence of the tailored Green's function, based on trigonometric functions, to represent the acoustic near-field.

Figure 2(c) shows the dipolar contribution to the total field of Figure 2(b), i.e. obtained by applying (9) without the quadrupolar incident field. Similarly, Figure 2(d) shows the contribution of the quadrupoles $\rho_0 v_i v_j$ only. We observe that the dipoles contribute only to approximately 1/5th of the total field, though the quadrupole only does not suffice by itself to obtain the correct pressure pattern. The importance of the quadrupole contribution is to be related to the relatively high Mach number, making the source region substantially non-compact. Moreover, the dipoles merely represent in this straight duct case the mirrored reflections of the quadrupoles, and have thus at most a similar acoustic efficiency. It is notorious that the dipole contribution dominates the quadrupolar one for more complicated geometries, in presence of geometrical features having small radius of curvature in comparison with the size of the turbulence source [8], a fortiori at lower Mach numbers.

Finally, Figure 2(e) shows the acoustic field obtained by scattering the source of Lighthill's Equation (1), i.e. the double divergence of Lighthill's tensor herein approximated as $\partial^2 \rho_0 v_i v_j / \partial x_i \partial x_j$ and accordingly regarded as a monopole. This result displays an acoustic field having a four orders of magnitude error with respect to the reference simulation. This highlights a fact already demonstrated many times: the dramatic fragility of the acoustic analogy when the correct multipole order is not imposed by the formulation. Though exact from a formal viewpoint, Eq. (1) expresses the source as a distribution of monopoles, with the result that numerical errors behave as monopoles as well and are therefore much more efficient radiators than the desired quadrupole field known to remain as leading order once all the source cancelations have been accounted for.

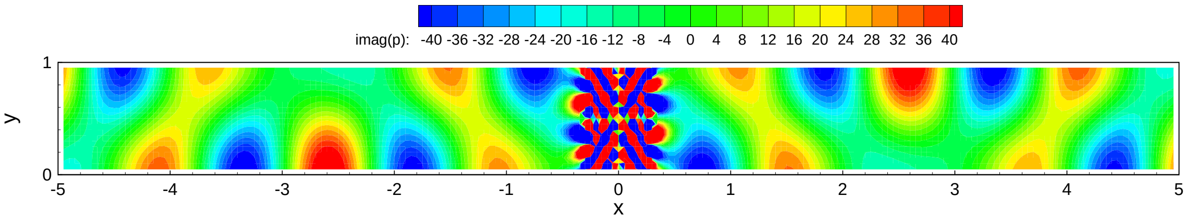

(a) Using tailored Green's function.

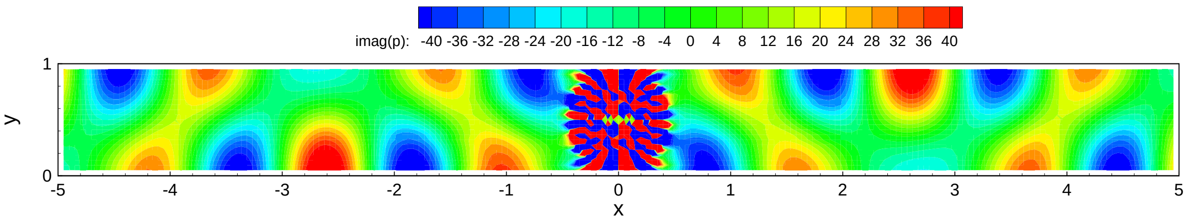

(b) Dipoles and quadrupoles using new formulation (9).

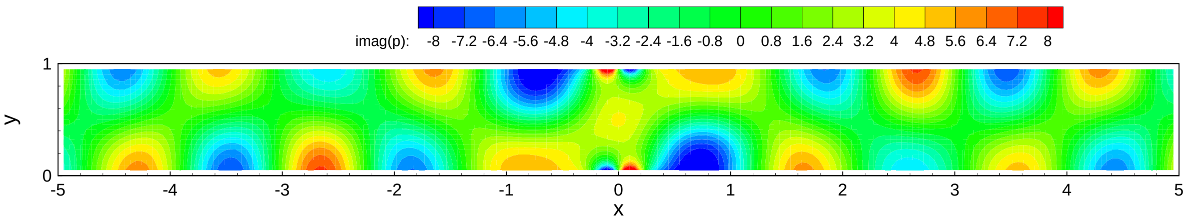

(c) Dipolar contribution alone.

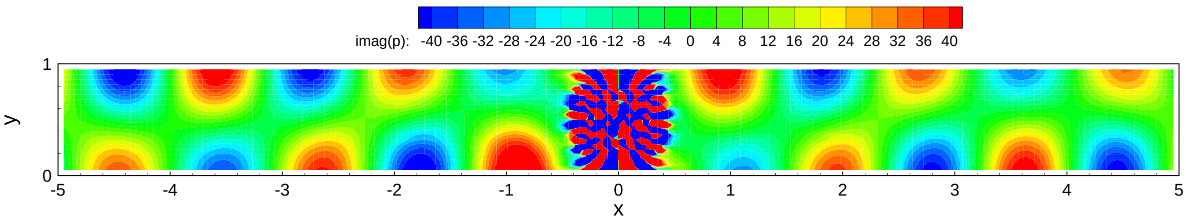

(d) Quadrupolar contribution T_{ij} alone.

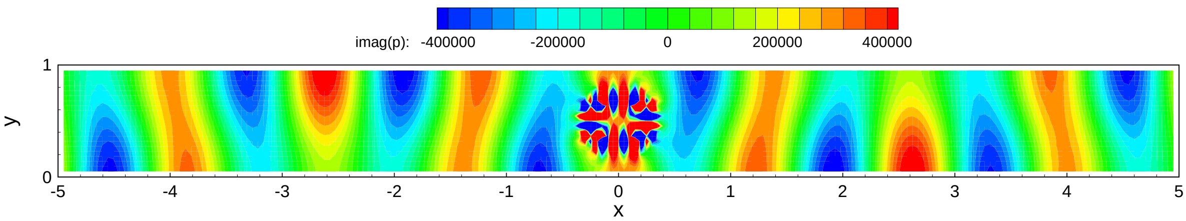

(e) Using monopole sources $\partial^2 T_{ij}/\partial y_i \partial y_j$.

Figure 2. Sound pressure field obtained for a frequency of 261 Hz ($k\,h = 4.8$).

4. CONCLUSIONS

An innovative approach, combining the Boundary Element Method with Curle's analogy, has been implemented in the BEM solver of the commercial code SYSNOISE Rev 5.6. It has been validated by application to a somewhat severe test case: the sound produced by the leapfrogging of a vortex pair in an infinite duct. The flow model and acoustical response of the duct can be derived quasi-analytically, leading to a reference sound prediction. The results obtained by our new BEM/Curle approach show an excellent agreement with the reference calculation, for a frequency above the cut-off frequency of the duct.

Another important conclusion is the spectacular failure of the analogy when considering the source field as a distribution of monopoles. Though theoretically exact, the convolution of this monopolar field with a free field Green's function yields errors in the acoustic prediction having a monopolar order also. At the opposite, Curle's analogy enforces the correct radiation efficiency of the volumetric source term, and yields an accurate prediction.

In summary, our method permits solving the acoustic propagation in geometries with arbitrary extent and complexity, exploiting the computational efficiency of Curle's analogy. Moreover, our method allows using an incompressible model of the flow field, which is a significant asset considering the stiffness issues faced by compressible flow solvers at low Mach numbers.

Acknowledgements The authors are grateful to the Flemish Institute for scientific and technological innovation in industry (IWT) for their support, provided in the framework of the project CAPRICORN (contract SBO 050163).

REFERENCES

[1] M. J. Lighthill. On sound generated aerodynamically. Part I. General theory. *Proceeding of the Royal Society of London*, A211:564–587, 1952.

[2] N. Curle. The influence of solid boundaries upon aerodynamic sound. *Proceeding of the Royal Society of London*, A231:505–514, 1955.

[3] M. S. Howe. *Theory of Vortex Sound.* Cambridge Texts in Applied Mathematics. Cambridge University Press, Cambridge, 2003.

[4] O. von Estorff, editor. *Boundary Elements in Acoustics – Advances & Applications.* WIT Press, Southampton, 2000.

[5] S. W. Rienstra and A. Hirschberg. *An Introduction to Acoustics.* Available online on http://www.win.tue.nl/ sjoerdr/, 2006.

[6] C. Schram and M. Tournour. Two-dimensional in-duct vortex leapfrogging as a validation benchmark for internal aeroacoustics. In *Proceedings of the 13th AIAA/CEAS Aeroacoustics Conference and Exhibit*, number 2007-3565, Rome, May 21–23, 2007.

[7] C. Schram, J. Anthoine, and A. Hirschberg. Calculation of sound scattering using Curle's analogy for non-compact bodies. In *Proceedings of the 11th AIAA/CEAS Aeroacoustics Conference and Exhibit*, number 2005-2836, Monterey, CA, May 23–25, 2005.

[8] M. Roger. Aeroacoustics: some theoretical background – The acoustic analogy. In J. Anthoine and T. Colonius, editors, *Computational Aeroacoustics*, volume LS 2006-05. von Karman Institute, Rhode-St-Genèse, 2006.